

Extending Wide Area and Virtual Reference Station Networks Far Into the Sea With GPS Buoys

Oscar L. Colombo, *GEST/NASA Goddard*
Manuel Hernandez-Pajares, Miguel Juan, and
Jaume Sanz, *Universitat Politecnica de Catalunya, Barcelona*

BIOGRAPHY

Dr. Oscar L. Colombo works on applications of space geodesy, including gravity field mapping, spacecraft orbit determination, and precise positioning by space techniques. He develops and tests techniques for precise very long baseline differential and point-positioning kinematic and static GPS, in collaboration with groups in the USA and abroad.

Dr. Manuel Hernández-Pajares is associate professor of the Technical University of Catalonia (UPC), from 1993. He started working on GPS in 1989, for cartographic applications. His focus is in the area of GNSS ionospheric determination and GPS Modernized and Galileo real-time positioning techniques.

Dr. J. Miguel Juan Zornoza is an associate professor of the UPC. His current research interest is in the area of GPS ionospheric tomography, and precise radionavigation.

Dr. Jaume Sanz Subirana is an associate professor of the UPC. His current research interest is in the area of GPS and Galileo precise navigation, and of Space Based Augmentation Systems (SBAS) processing algorithms.

ABSTRACT

We have studied the potential of using buoys with GPS receivers as floating network stations, to extend, far into the sea, the navigation services offered by land-based WAAS/EGNOS and Virtual Reference Station networks.

In particular, we have investigated the feasibility of real-time resolution of carrier phase ambiguities with a roving receiver hundreds of kilometers away from shore. Central to that resolution, is the modeling of the ionosphere using data from both land- and buoy-based GPS receivers in the network, particularly in the presence of Traveling Ionospheric Disturbances (TID) and other perturbations, and of occasional interruptions in buoy receiver operation, with complete loss of lock lasting several minutes. Establishing precise kinematic location of the buoy quickly at start-up, and recovering it soon after an interruption in GPS reception, are essential to the use of buoys as effective aids to precise navigation. Ways of speeding up the real-time convergence of the buoy's estimated position in such cases are discussed in this paper.

In our preliminary tests, we have used 5-second GPS data from widely spaced NGS CORS stations, from days with low and quite high ionospheric activity. One of them, situated eastwards from all the others, was used in lieu of a buoy, and positioned kinematically relative to the "fixed" sites, while contributing data to precise, Virtual Reference Station ionospheric differential corrections, and to WAAS-type ionospheric models. Other receivers were kept in reserve, to be treated as user "rovers", also positioned kinematically. We then considered the quality of the ionospheric corrections, from the point of view of fixing the "rover" ambiguities relative to the "master" station. The estimated rates of successful ambiguity resolution attempts are comparable to those for conventional, land based Virtual Reference Station and DGPS networks of smaller size. The quality of the corrections of the ionosphere derived from models obtained by computed tomography is adequate, in particular, for WAAS/.EGNOS-assisted navigation.

INTRODUCTION

Virtual Reference Station (VRS) [1], [2], [3] and Wide Area (WA) [4], [5] techniques rely on networks of GPS stations to assist real-time GPS navigation both within and just outside their perimeters. VRS and WA networks differ in their typical inter-station distances: 50-150 km, and 300 – 1000 km, respectively, and in their main purpose. WA networks (WAAS, EGNOS, etc.) chiefly support meter-level real-time navigation, with very robust integrity of service monitoring, primarily meant as an aid to civil aviation and other uses where safety of life is a paramount issue. There are some higher precision wide area services available for less safety-critical applications, and future ones being studied, for example, by government agencies such as the US Coast Guard. On the other hand, the denser VRS networks are intended for very precise navigation and surveying where safety-of-life is not a major issue. Until now, precise network-based services have been effective mostly on land areas and the airspace above. In some cases, they may also cover adjacent seas up to some tens of kilometers from the coast. Oil platforms and similar offshore installations could, sometimes, be used as additional network stations, to extend the service further out, but they are available in relatively few places.

Moored buoys used as network stations would be different from conventional, fixed land stations, in that their locations could not be considered already known, but would have to be found continuously and precisely in kinematic mode, as waves, currents, and tides move them about, even if they are anchored to the seafloor.

Already, buoys with GPS receivers on board have been positioned precisely, repeatedly, and reliably, during sessions ranging from several hours to many days, for a variety of purposes, such as satellite altimetry calibration-validation [6], [7] or the development of tsunami detection systems [8]. Most of this work has been done with buoys within 10-20 km of a GPS land station, using conventional short-baseline classical differential or VRS procedures [9]. However, there is no reason why GPS buoys cannot be positioned reliably, and with great precision, much further out at sea, and in real time. Doing so would greatly increase the scope of their present applications. Tsunamis could be detected much earlier, to warn populations at risk, giving well in advance of their arrival on land, giving them a better chance to escape with their lives. It would make possible to use such buoys as GPS network stations deployed far into the ocean. This could, eventually, add many tens of thousands of square kilometers to the areas where such networks support sub-decimeter navigation. With effective L1 and L2 ambiguity resolution, such level of precision could be available within a few minutes of turning on an onboard GPS receiver on a ship or an airplane, even when quite far from land. At present, under such conditions, it is often

necessary to wait for half an hour or more, while estimating the biases of the ionosphere-free combination of the L1, L2 carrier phases (Lc biases), before achieving the desired precision.

To be part of an effective and safe service, GPS buoys and their equipment have to operate continuously and reliably in a difficult environment, and also survive well enough to be repaired and put quickly back into service, in spite of the worst the sea can throw at them: twenty-meter freak waves, typhoons and hurricanes. They also have to cope with less dramatic, common problems such as corrosion, barnacles, and even perching sea-birds. Finally, the buoys have to be in continuous contact by radio with their WA or VRS network's main processing facility, transmitting to it GPS data and other information, such as telemetry, and receiving from it operator commands. This means using satellite links and bandwidth-saving compression techniques. All these problems are being addressed as part of existing projects involving GPS positioning of buoys in the high seas. Long-lasting, reliable open ocean buoys (without GPS) have been deployed, continuously, for years, carrying oceanographic instruments, and in support of NOAA's tsunami detection system based on seafloor pressure sensors. Also, the communications aspects of VRS and WA services are already well developed and understood. Therefore, we have chosen to concentrate here on the GPS data analysis and, in particular, on the treatment of ionospheric delays.

Buoys built to function for prolonged periods of time unattended, far from land, are of necessity large and expensive. Giving them more than one application, for example of detecting tsunami and serving as aids to precise and safe navigation, would make them more likely to be deployed, both to assist commerce, engineering, and scientific purposes, and to help save lives.

To test our ideas, we have used some 15 hours of continuous 5-second GPS data downloaded, via the Internet, from several NOAA's CORS stations separated by hundreds of kilometers. We have processed those data both during periods of low and high ionosphere activity, treating in each case two of the sites kinematically, one as a moving "buoy station", another as a "ship" sailing within or near the perimeter of the land-and-buoy network while using the corrections provided by it, and the rest as conventional, fixed land stations.

We have considered the case where the buoy is to the East of the land stations. This situation is the least favorable for the proper modeling of the ionosphere. The ionosphere's electron concentration, modeled in three dimensions by computed tomography [10], [11], [12] using dual-frequency data from all receivers in the network, including the buoy's, depends largely on the local position of the sun in the sky. The patterns of electron concentration tend to drift, therefore, from East to West at a rate of 15 degrees per hour (or about 1000

miles per hour at the Equator). With no GPS receivers east of the buoy, the ionospheric model tends to be weakest in that direction. This could affect adversely the resolution of carrier-phase ambiguities for the rover, and also of the buoy. The latter is essential, because the buoy's data are needed for making some of the unambiguous differential ionospheric corrections relative to a master land station that are then interpolated to the rovers.

So establishing precise kinematic location of the buoy quickly at start-up, and regaining that precision soon after an interruption in GPS data, are both essential to the use of buoys as effective aids to precise navigation.

TECHNIQUE

Refraction Corrections: The corrections transmitted to the user from the operations center of a differential, VRS or WA network, may include, in one form or another, ionosphere and troposphere delay information. The user's software calculates the corrections at the location of the rover, and applies those to the rover's receiver data. So both types of correction involve: (a) creating and updating a model based on GPS data from the network (b) computing corrections based on that model. Each step involves some error, the sum of which affects the user's results. The precision of step (b), which usually involves a spatial interpolation from the network stations to the rover, depends on the "lumpiness" of the ionosphere and troposphere delays. That is to say, on how much they depart from smooth functions of position within the area served by the network. In general, the troposphere is likely to be the less smooth, and have worse interpolated results, in networks with large inter-station distances. This can be taken care of if the troposphere correction is calculated by the user's navigation software, instead of being transmitted to it, as in VRS. That is a feature available in some navigation programs, including the one (developed by the first author) that we have used for the kinematic part of our work.

Ionospheric Model: First, a computed tomography model of the ionospheric Total Electron Content (TEC) is obtained using data from all GPS receivers in the network, including the buoy. As described, for example, in [11], our model consists of two spherical shells, both divided into three-dimensional cells, or voxels, each assumed to have a spatially constant electron density that changes slowly over time, since the spherical grid is sun-fixed. All these voxel densities are estimated with a Kalman filter, along with the effect of carrier-phase ambiguities and receiver and satellite hardware delays. Only active cells (with actual GPS data to estimate their electron densities) are solved for at each filter update, to speed up calculations. The Kalman filter is updated once every five minutes. We have used this type of model successfully in a number of demonstrations of ambiguity fixing over very

long baselines. It can be used directly, to remove the effect of the ionosphere from L1, in WA (e.g., WAAS or EGNOS) assisted navigation, or indirectly, to help obtain centimeter-level differential corrections for VRS and similar forms of very precise navigation, so users can resolve their carrier-phase ambiguities. The computer implementation of the modeling algorithm is efficient enough to be used in real time, with an ordinary modern PC. The data are L1 and L2 GPS carrier phase and pseudo-range. Following the Wide Area RTK (WARTK) technique, described in [16], the estimated parameters are:

- The electronic content in each voxel of a three-dimensional mesh of 300km x 300 km in latitude and longitude, arranged in two concentric spherical shells with bottom, mean and top heights of: 60 km, 740 km, and 1420 km, respectively.
- The biases in the ion-free combination L_c and in L1 floated and fixed, whenever L1 and L2 can be fixed.
- Satellite and receiver clocks.
- DCBs, or instrumental delays in the satellite transmitters and in the receivers.
- Tropospheric zenith delays for the receivers.

Resolving Ambiguities: (a) Fixed Sites. For very precise navigation, the purpose of the model of the ionosphere is to help resolve the ambiguity of carrier-phase data double-differenced between the stations in the network, beginning with the widelane.

For that to be successful more than 95% of the time, the combined effects of the ionosphere, GPS orbits, station position errors, and tropospheric refraction should be calculated with a standard deviation uncertainty of less than a quarter of a widelane cycle (< 22 cm). Once this is done, and if the L_c biases are known with a one-sigma precision of better than 2.7 cm (one quarter of a narrowlane cycle), it becomes possible to resolve the narrowlane with approximately 95% confidence, and thence L1 and L2. With fixed receivers on carefully GPS-surveyed land sites, the resolution of ambiguities between sites is possible because the network receiver locations are known to better than one inch in a global reference frame, the effect of tropospheric refraction on the propagation of signals at the site can be estimated to better than two centimeters, and the errors in GPS orbits are usually not an issue with baselines of less than 400 km with reasonably precise orbits, such as can be obtained by refining broadcast orbits with data from the supporting local or global network [15], [18], [19], [20], and the orbit errors and wet troposphere zenith delay are included among the unknowns of the network solution. With the widelane and L_c biases already known well enough to resolve the narrowlane, one can get the exact L1 and L2 ambiguities. With these, one can calculate the ambiguity in L1, the difference between the L1 and L2 phase ranges, which is also a measure of the Slant Total Electron Content (STEC). Finally, this observable, double differenced (ddSTEC) relative to a master reference

station, is interpolated to the approximate user location. This is usually done (in VRS, for example) by transmitting to the user the ddSTECs for the baselines between various stations in the net and the master station, along with other corrections. The user's software then interpolates them to the rover's approximate location (calculated with pseudo-ranges).

(b) Buoy. The situation is more complex when one of the sites is not fixed, but is moving with tides and currents, as a buoy would, even when it is well anchored.

In this case, one cannot rely on a previously surveyed location, but has to estimate continuously the position of the buoy with a kinematic technique. This has to be achieved well enough so the Lc biases are known with a precision better than 2.7 cm, so they can be used as described for the fixed land sites.

Feed-Back to Tomographic Model. Once obtained, the unambiguous ddSTECs for all satellites and all baselines between network sites (buoy included) and the master station, are used to constrain the unknown STEC biases while modeling the ionosphere, which improves the precision and speeds up the convergence of the model's Kalman filter. All this takes place in real time.

Constraining the Kinematic Solution. To achieve quickly, and maintain, the necessary location precision, the kinematic solution can be improved by taking advantage of one basic fact about buoys: they float in the sea. While the instantaneous sea surface height, and that of the buoy, changes up and down, with passing waves, by as much as several meters, these are more or less regular oscillations with periods rarely exceeding 15 seconds. On the other hand, the instantaneous mean sea level, obtained by smoothing out the wave action, changes very gradually. This can be used to constrain the solution, as described in more detail in [13]. Briefly, the carrier phase data are averaged over periods of (in this study) two minutes, and the mean sea height for the same period is estimated from these averages. This mean sea height is represented by a random walk with a system noise corresponding to the expected rate of change in geocentric sea level due to local ocean and solid earth tides, wind pile-ups, variations in air pressure, etc. Much of that can be modeled and used to correct the data at the decimeter-level, so the constraint is actually applied to the residual mean sea height, which changes less, and more slowly, than the original mean sea height.

(c) Rover. To test the ability of a network that includes a buoy to support precise navigation, we tried resolving the ambiguities of a roving receiver with the technique used in previous tests, as described in [10] and [12]. It is a geometry-free, non-iterative technique, designed for very long baseline differential GPS. First, the precise, unambiguous ddSTEC between at least two network stations, (the buoy being one of them) and the Master Reference Station, are received from the network control

and computation center and interpolated to the approximate position of the roving receiver. The error in this interpolated value should be less than ± 2.7 cm, for exact ambiguity resolution. First, the value of the rover/Master or Virtual Station double-differenced Lc, minus its bias, estimated with the user's navigation Kalman filter as a "floated ambiguity", is subtracted from the widelane, along with the corresponding ionospheric correction, using the interpolated ddSTEC. If the error in the estimated Lc bias is less than 22 cm, the widelane can be resolved. With this ambiguity known, that of LI can be determined after correcting LI with the interpolated ddSTEC, to get a noisy value of its ambiguity, which can be made more accurate by averaging it over several epochs. Once both the widelane and the LI ambiguities are known, those of L1 and L2 can be obtained immediately. Now, the Lc bias can be calculated exactly. After some checks for parity agreement between wide and narrow lanes, proximity of noisy ambiguities to an integer number of cycles before round-off, etc., the Lc bias can be assimilated in the filter as a pseudo-observation with a small uncertainty, but only if the precision of the "floated" Lc is not high enough yet (worse than 2 cm). Once assimilated, a null-hypothesis test of the a posteriori pseudo-observation residual can be made, to accept or reject it. This is a fairly robust procedure. Because Lc is not fixed exactly, but continues to be updated or "floated", it is possible to tolerate errors in the interpolated ddSTEC correction as large as ± 8.1 cm, which results in errors of ± 11 cm in Lc. Such errors can be absorbed by the solution with little ill effect, if they are not too frequent and numerous, provided that the pseudo-observations are not weighted too heavily. Finally, it is enough to resolve three double-differences to achieve decimeter-level precision.

The downside is that it may take from several minutes to more than half an hour to get Lc resolved with sufficient precision to start the process, depending on satellite geometry. The mean sea level constraint, and the use of the phase reconnection scheme described next, can help shorten this delay, as can also the use of low-multipath pseudo-range, treated as a separate data type, in addition to the carrier phase.

There are many other ambiguity resolution techniques, some considerably faster than the one we have used for this preliminary study, which will become much faster once three-frequency GNSS becomes reality [14]. It is known that, for distances of less than 100 km between receivers, typical of VRS, the usual integer search methods for fast ambiguity resolution can be useful. With larger area networks, poor accuracy in the interpolated tropospheric corrections could be an obstacle, requiring navigation procedures that also solve for the zenith delay at the rover. The one we have chosen belongs in this category.

Recovery after Breaks in Reception. Introducing the mean sea level constraint in the kinematic solutions for the buoy and the rovers speeds up the convergence of the navigation Kalman filter and, therefore, that of the Lc biases needed to resolve the carrier phase ambiguities, particularly those of LI. Sometimes, with poor geometry (large PDOP), convergence to decimeter-level precision may take well over half an hour. So, once the filter has finally converged, it is imperative to maintain its final precision for as long as possible. An interruption in reception for whatever cause, if long enough, would require a restart of the filter, so the buoy will be out of service, and, or a user will be unable to have precise results, for as long as the interruption lasts, plus the time it takes for the filter to fully converge again afterwards. A key issue in keeping the convergence time to a minimum is to reestablish phase continuity in LI as soon as possible. We have studied a geometry-free procedure derived from the one we have used to resolve the rover ambiguities, replacing the words “ambiguity”, “Lc bias”, and “LI”, for “ambiguity change”, “Lc bias change”, and “LI change” (across the data gap). This procedure can be used also in point positioning, or even when no network ionospheric corrections are available. The first step is to find the widelane ambiguity change after the gap, which requires knowing the change in LI. We have tried several simple ways of calculating that change, and settled for fitting a parabola to both the last six minutes of LI observations before the gap, and to the mean speed of change in LI over a few epochs after the gap. The results were satisfactory with both low and high levels of ionospheric activity, for gaps as long as five minutes. For L1 and L2 to be fully resolved, the change in Lc has to be estimated to better than 22 cm (half a widelane cycle), which could take several minutes, but the unambiguous value of LI is known already a few epochs after the gap. So, in the case of the buoy, it can resume providing unambiguous ddSTEC information for updating the ionospheric model and corrections without waiting for the widelane and LI to be fixed as well. Since over a few minutes, changes in wet troposphere zenith delay and in mean sea level can be quite small, it is possible to speed up convergence further by restarting their error states in the filter with the same values and precision they had before the gap. A third GNSS frequency will make it possible to fix all ambiguity changes in a few epochs [16].

Integrity Monitoring of Ionospheric Corrections.

The variability of the free-electron content in the ionosphere depends on the level of geomagnetic activity (measured, for example, with the Kp index), as well as on the season of the year, the local time of day, and the magnetic latitude of a particular place. This variability is usually measured as the rms of a time series of quantities reflecting the effect of the ionosphere on the propagation of radio waves. In the case of VRS networks, some measures are based on the rms variability of the STEC

gradients used to interpolate linearly the ddSTEC from the network sites to user locations, or on the rms difference between actual and interpolated ddSTEC in a test baseline [1], [3]. As in some previous work [16], we have adopted here a simpler measure of variability that can be calculated either with network receiver data, and transmitted to the users, or by the users with data from their own receivers (receiver autonomous integrity monitoring, or RAIM). This is the rms of the curvature D_LI of the STEC for each satellite, from the observed L1 and L2 carrier phases:

$$D_LI(t) = LI(t-300) - 0.5[LI(t) + LI(t-600)]$$

where t is the epoch, in seconds, and LI is the difference between the observed L1 and L2 phase ranges, in meters. The rms of D_LI, calculated over a sufficiently long interval, such as the last 1000 seconds, is the Single Receiver TID Index, or SRTI. A Traveling Ionospheric Disturbance, or TID, is a common and troublesome disturbance that propagates in waves across the sky, causing more or less sinusoidal oscillations in STEC and in the GPS ranges, with periods of 10-60 minutes (medium scale TIDs) or longer, and up to decimeters in amplitude. This index, monitored at the stations of the network, could be used to detect and edit out satellite data seriously affected by TIDs, so that is not used in the ionospheric model or the user corrections

TESTS

Test Setup. The tests were meant to determine the value of adding a moving receiver (buoy) to a conventional VRS or a precise DGPS network of fixed receivers. We also assessed the quality of the un-differenced STEC from the tomographic model, to establish their potential usefulness in WA (WAAS/EGNOS-type) applications. For this preliminary feasibility study, lacking actual buoy data, we have used 5-second, dual-frequency GPS receiver data from several NGS Continuously Operating Reference Stations (CORS) in the central and southern USA. Along with the data, we downloaded from the Internet precise coordinates for the sites, including those treated as the buoy and the rovers, against which we compared the kinematic “real time” results. Those precise coordinates also made it possible to determine the true values in all baselines of the double-differenced carrier phase ambiguities. For that we used not only a Kalman filter, as in the simulated real time calculations, but also a smoother, both for the ionosphere modeling and the navigation solutions. The CORS stations chosen to form our test network are shown in Figure 1. The station MCON was selected as the “buoy”, STKR and PKTN, as possible “rovers” (so their data was kept in reserve, and not used to model the ionosphere). The data were from two different days, one with low and one with high ionospheric activity (Fig.2).

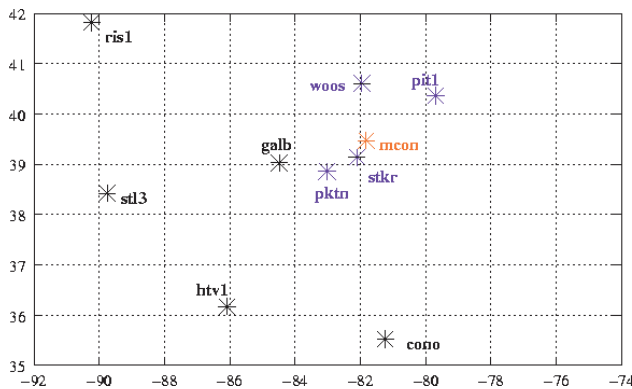


Figure 1 The test network was made of NGS CORS sites. GALB is the master reference site, MCON, the “buoy” site, and STKR and PKTN are “rovers”. RIS1 was not used on day 130. Outside the network’s perimeter, WOOS and PIT1 were used in tests of the ionospheric model for EGNOS/WAAS applications.

While all stations contributed data to the computed tomography model (used to resolve the widelane ambiguities between network stations”) For the interpolation of the unambiguous ddSTEC to the position of a “rover”, was used data from the baselines: between GALB (the Master Station, in Galbraith, Ohio) and MCON (the “buoy”, actually a site in McConnelsville, in Ohio), and between GALB and CONO (in Conover, North Carolina). The “rover” were situated in Piketon, Ohio (PKTN), and Stocker University, in Athens, Ohio (STKR) The lengths of the baselines between the various sites and GALB are listed in Table 1.

TABLE 1

Distances from Master Station to the Rest of the Network

GALB to RIS1 #	576.345 km
GALB to STL3	462.058 km
GALB to HTV1	346.908 km
GALB to CONO *	484.114 km
GALB to MCON *	234.016 km

Distances from “Rover” Sites to GALB

PKTN to GALB ++	127.693 km
STKR to GALB	205.620 km

Distances from “Rover” Sites to “Buoy”

PKTN to MCON	123.615 km
STKR to MCON	44.195 km

* Baselines used to interpolate unambiguous ddSTEC corrections to “rover” sites.
 ++ Used only on day 130 # Used only on day 191.

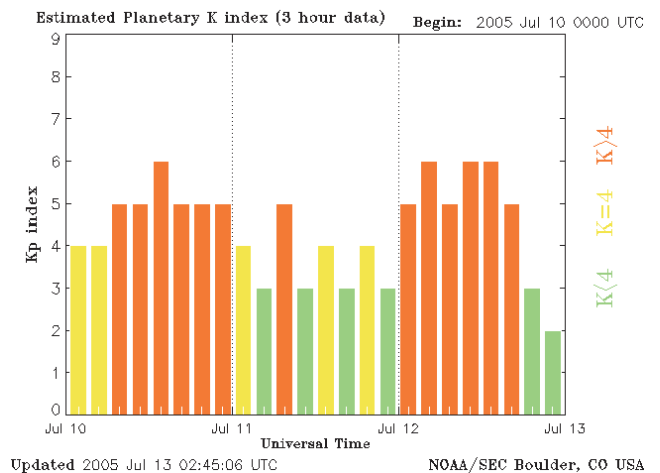
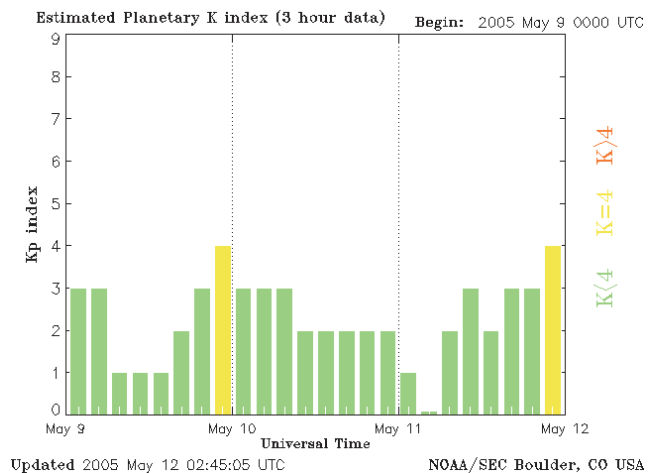


Figure 2 Plots of ionospheric activity (from NOAA Space Environment Center) that include days 130 (10 May) and 191 (10 July) of 2005. Planetary K index (Kp): Green bars indicate low ionosphere activity; amber, elevated; red, high (here, with probable occurrence of minor geomagnetic storms).

For GPS orbits, we used the non-predicted part of the ultra-rapid IGS orbits for each day, keeping them fixed. The idea was to use something less precise than the final IGS orbits, which could be obtained by correcting the broadcast orbits with data from the network itself [15].

Days 130 and 191, 2005. We chose the 5th of May (day 130), because of the very low level of geomagnetic activity, and the 10th of July of 2005 (day 191), because of the higher level. In total, we analyzed some 20 hours of data from each day. It took several of the earlier hours for the tomographic ionosphere solution to converge, and then close to 30 minutes for the navigation filter for the “buoy” to achieve the required decimeter-level precision. These delays would occur only during a complete “cold start” of the system; normally, both network-related filters should run uninterrupted for many days, with very

occasional fast “warm-restarts” for the buoy (see previous section on “Recovery after gaps in reception”, and also Fig. 11, and its explanation in “Results”, below). As the baseline double-differenced ambiguities, including those of the “buoy” were resolved, the corresponding unambiguous ddSTEC were obtained and: (a) fed-back to the ionosphere modeling, to strengthen its results; (b) those for the baselines GALB/MCON and GALB/CONO were interpolated linearly to the GALB/PKTN and GALB/STKR “rover” baselines, in the manner described in [16], to get precise estimates of their ddSTEC. These

were then used to correct out the effect of the ionosphere from the “rover” data, and resolve the GALB/rover double-difference ambiguities in “real time” (that is to say, using only the navigation Kalman filter, without smoothing). The main difference between these two days were the levels of geomagnetic activity, the use of station RIS1 only on day 191, and the availability of 5-second data for the “rover” site PKTN only on day 130. The test results are illustrated in Figures 3 – 16 below, and discussed in the next chapter.

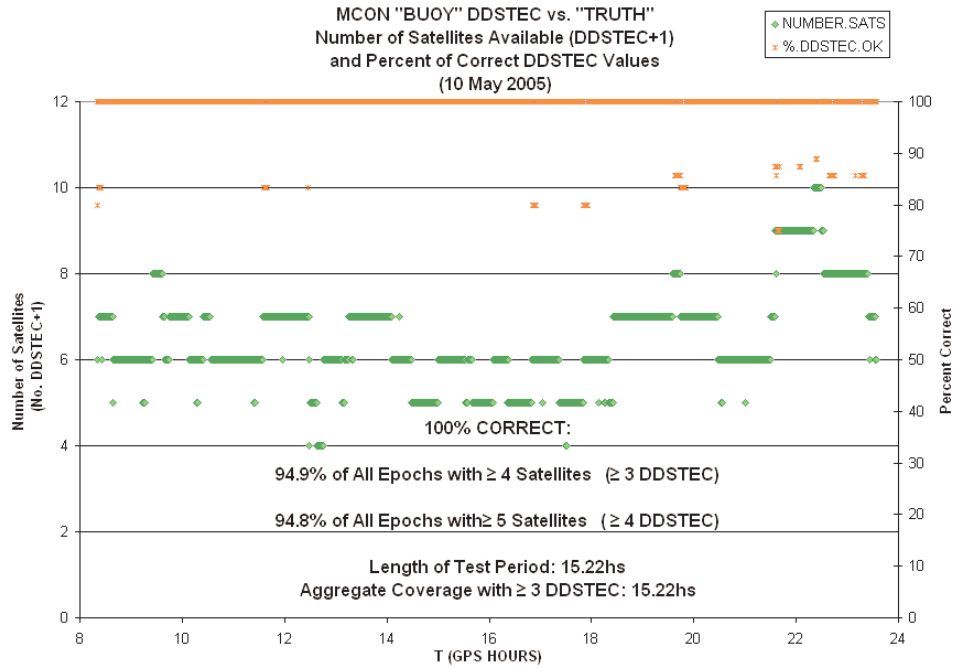


Figure 3. Number of satellites with unambiguous ddSTEC for ionospheric corrections available from baseline GALB/MCON (“buoy”), and percentage of correct ones, at each epoch during day 130 test. (Elevation cutoff: 10 degrees.)

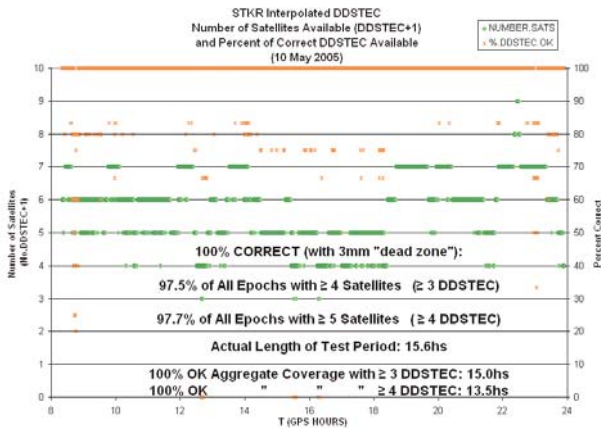


Figure 4. As in Figure 3, but for ddSTEC corrections interpolated to “rover” at STKR

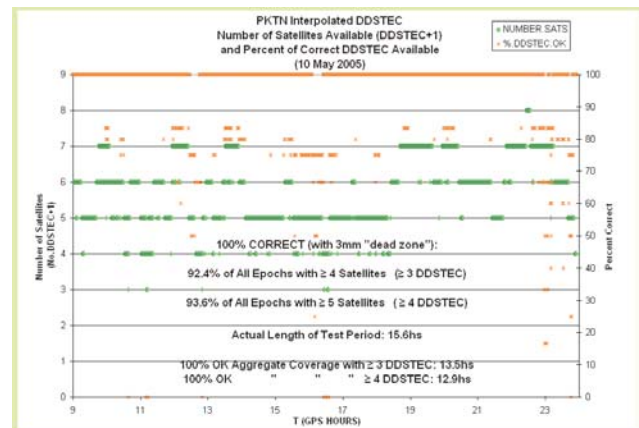


Figure 5. Same as in Figure 4, but for “rover” at PKTN.

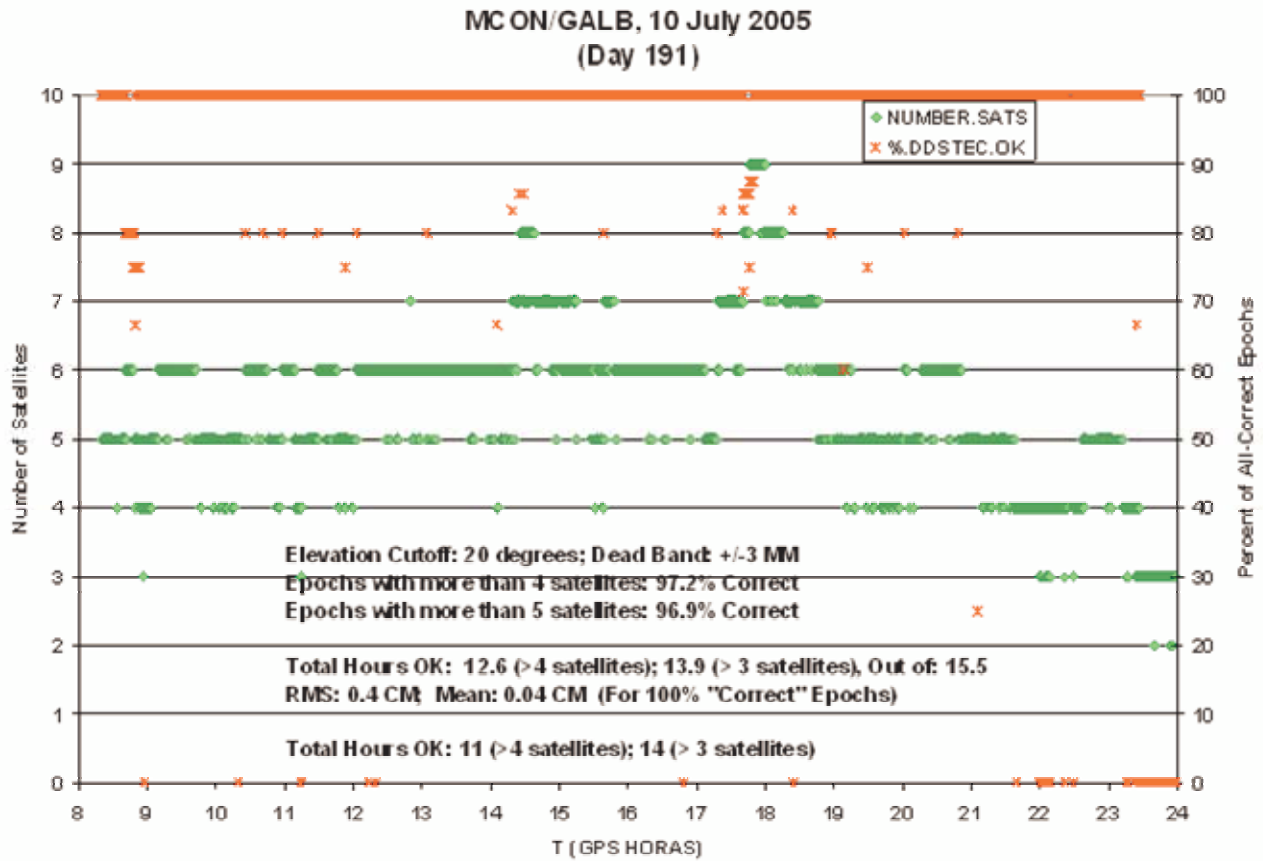


Figure 6. Same as in Figure 3, but for day 191, with a higher (20 degrees) elevation cutoff, to deal with the greater ionospheric activity. There were fewer or no satellites with corrections based on “buoy” data (0% red marks).

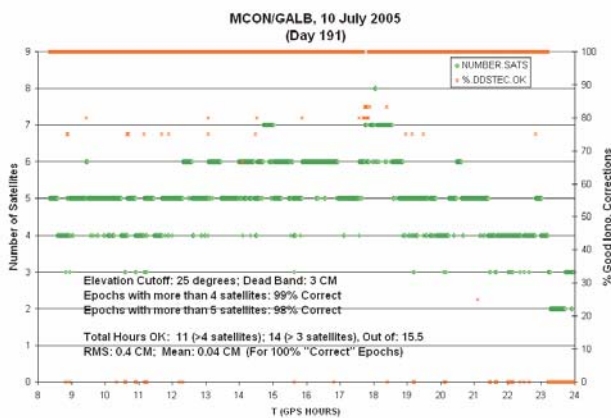


Figure 7. Same as Figure 6, but with an elevation cutoff of 25 degrees.

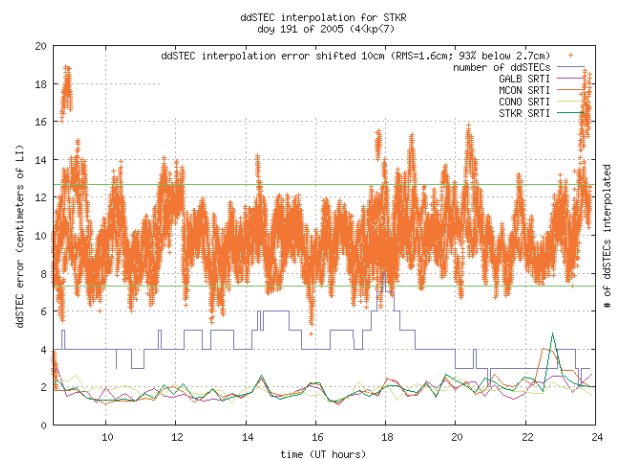


Figure 8. Day 191: STKR interpolation errors (shifted +10cm). Epochs with errors larger than +/-2.7 cm (green lines) will have incorrectly fixed ambiguities for baseline GALB/STKR. Notice correlation between larger errors and higher SRTI index (SRTI >2) at key stations.

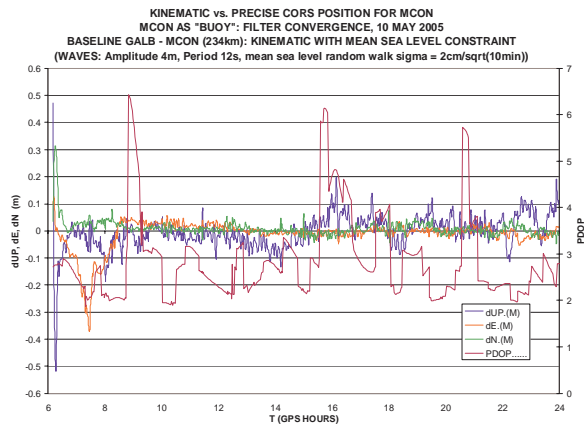


Figure 9. Convergence of Kalman filter-only (simulated “real time”) kinematic solution for “buoy”. RSS error should be (mostly) below 10 cm for procedure to work.

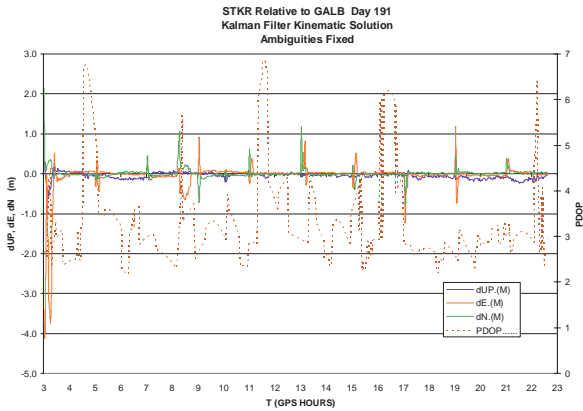


Figure 10. STKR “rover” Kalman filter convergence when using interpolated ddSTEC corrections to fix ambiguities. Filter re-started every 2 hours (notice additional, unscheduled re-start at 8:15 hours). Day 191.

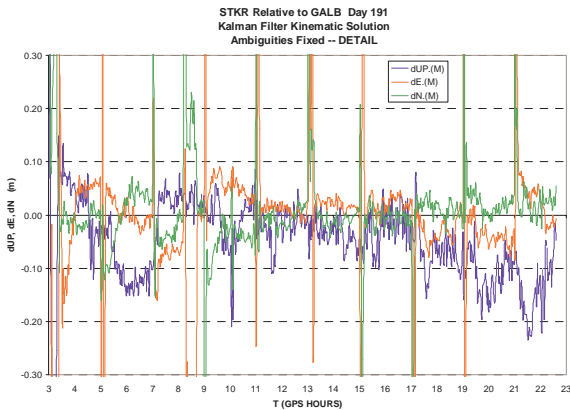


Figure 11. As in Figure 10, at a larger scale. Ambiguity resolution causes convergence within a few minutes of each restart, except between 8:15 and 8:45 hours, when no corrections were available because of poor conditions.

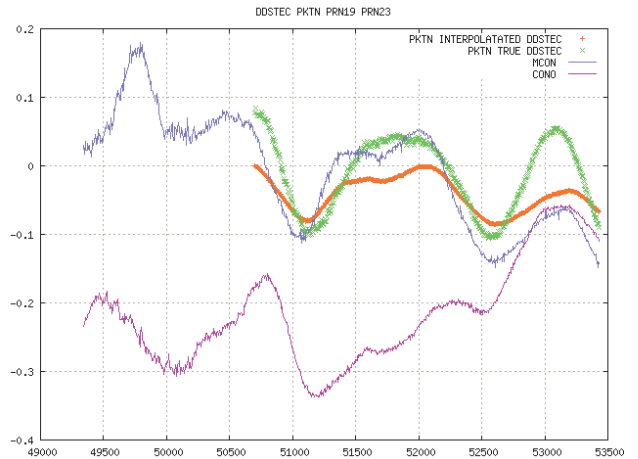


Figure 12. How TIDs affect adversely the interpolation of ddSTEC corrections to rover.

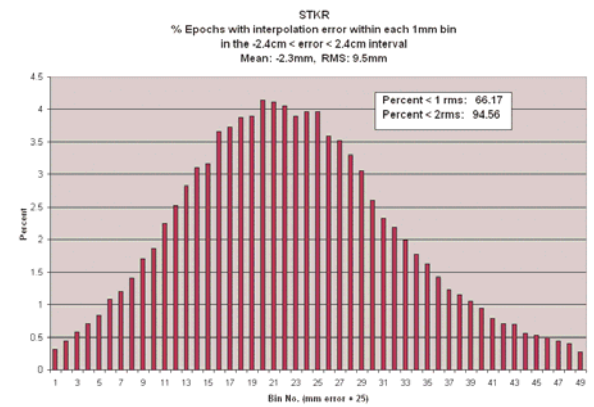


Figure 13. Histogram of errors in interpolated ddSTEC for STKR, day 130, compared to “truth”: post-processed values with exact (CORS) coordinates (shifted +25 mm).

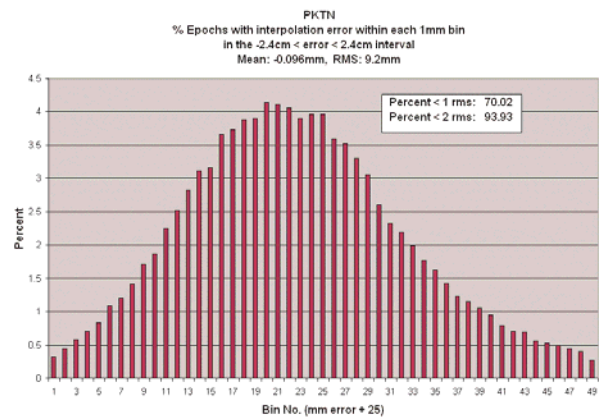


Figure 14. As in Figure 13, but for PKTN.

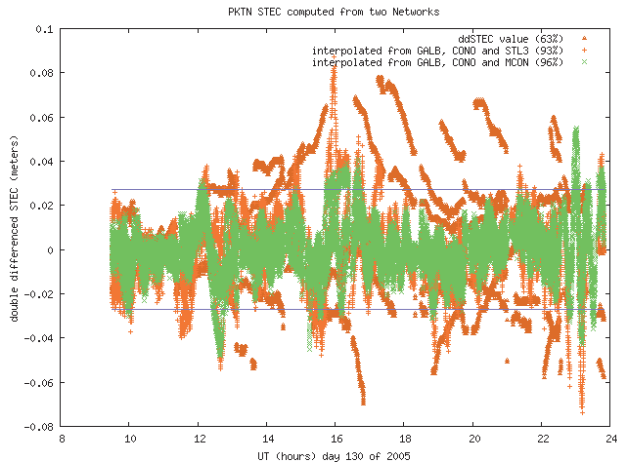


Figure 15. Day 130: Errors in ddSTEC corrections for PKTN with (green) and without (red) the “buoy” (MCON) station in the network. No correction: brown.

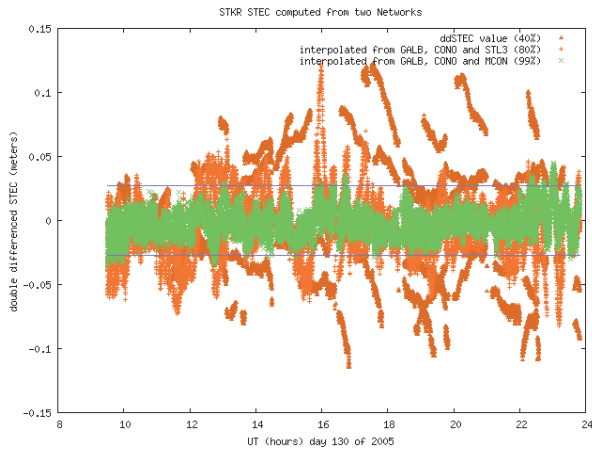


Figure 16. Same as in Figure 15, for STKR. Closest site to “buoy”, results here are most sensitive to its influence.

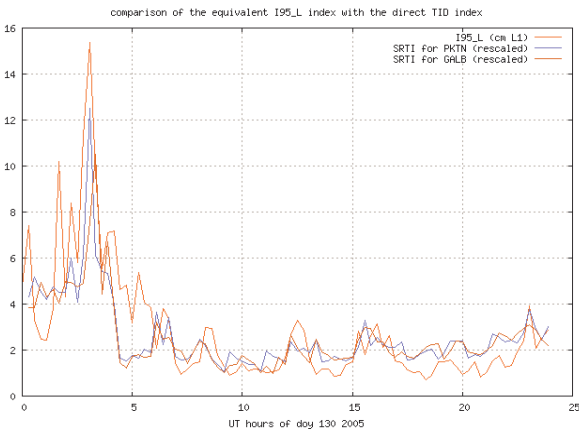


Figure 17. Comparison of the SRTI index, based on RMS curvature of observed ddSTEC, and the often used I95-L index, based on RMS residuals at a fixed test site.

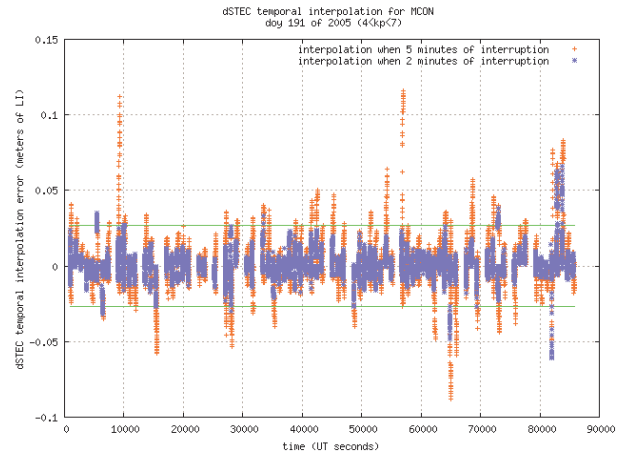


Figure 18. Errors in ddSTEC for MCON, day 191, when repeatedly interpolated across 2-minute (blue) and 5-minute (red) gaps in all satellite data. Successful interpolation (errors between green lines) means quick recovery of the position precision achieved before the gap.

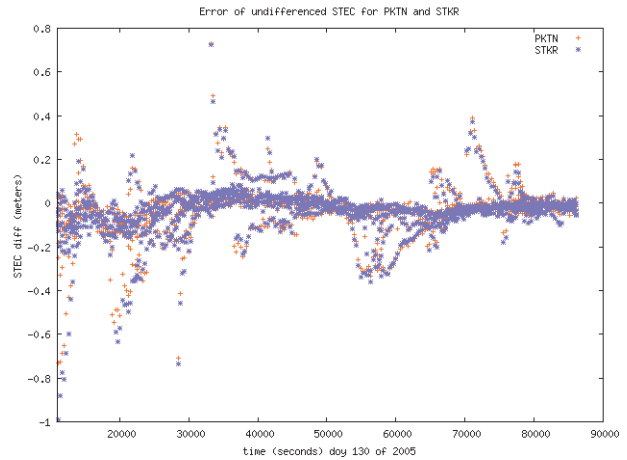


Figure 19. Errors in tomographic, undifferenced STEC for STKR (blue) and PKTN (red).

RESULTS

For day 130, Figures 3-5 illustrate the comparison between the unambiguous ddSTEC —determined at the “buoy” (MCON) and at each “rover” (STKR and PKTN) — and the off-line unambiguous ddSTEC (“truth”) determined using the filter and the smoother of the ionosphere modeling procedure, and the exact CORS site coordinates. The unambiguous ddSTEC for GALB/MCON were obtained as part of a kinematic solution with the navigation Kalman filter, in simulated real-time analysis. Most importantly, Figure 3 shows what difference it makes to have a moving site (buoy) instead of a fixed site (MCON) in a wide area network.

The ddSTEC for both STKR and GALB were interpolated to the GALB/STKR and GALB/PKTN (day 130, only) baselines from GALB/MCON and GALB/CONO. Shown in the plots with green diamonds are the number of satellites (number of ddSTEC+1) for which there are corrections available at each epoch. The red markings indicate the percentage of unambiguous ddSTEC obtained kinematically that are the same as those computed off-line, or truth. Also shown are the total number of hours in the intervals plotted, and the total coverage, also in hours, when all ddSTEC were correctly resolved or interpolated, as the case may be, that corresponded to four or more satellites in common view between the “Master Station” GALB, and the “buoy” MCON. This being a day of fairly quiet geomagnetic conditions, the satellite elevation cutoff was set to 10 degrees. The lower this cutoff, the more satellites in common view with the Master Reference Station, but the worse resolved and interpolated the ddSTEC for the lowest elevation satellites. We have found that the choice of elevation cutoff is an important part of the engineering compromise between availability and reliability of the ionospheric corrections.

The distinction between “more of 4 satellites” and “more than 5 satellites” is made for the following reason: many ambiguity resolution procedures require more than four satellites to work successfully. Our geometry-free technique, implemented as part of the navigation Kalman filter solution, works with just four satellites in common view (three double differences). However, until three-frequency GNSS become available, it will be slower than many geometry-dependent methods that need more satellites in common view. The “dead zone” mentioned in the plots is a band 6 mm wide centered at ± 2.7 cm. The residual ddSTEC in the baseline of the rover, after correcting with its interpolated value, is rounded off to the nearest integer number of cycles of LI, and the LI ambiguity is thus resolved, but only if the residual is within $\pm(2.7-0.3)$ [cm] from a whole number of cycles. The set of all candidate integer cycles of LI is determined once the value of the widelane ambiguity is known, which is why this is resolved first. Use of a “dead zone” increased the number of epochs with all ambiguities resolved correctly by several percentage points.

For day 191, Figures 6 and 7 display similar information as Figure 3 for GALB/MCON. Here the elevation cutoffs are at 20 and 25 degrees, respectively. Higher elevation cutoffs than those for day 130 were made necessary by the much higher geomagnetic activity. The two Figures show how, increasing the elevation increases the percentage of epochs where all the unambiguous ddSTEC are correct, but also decreases the number of double differences on which those corrections can be used.

Figure 8 shows the disagreement in STKR between interpolated and “true” ddSTEC (for all double differences). From this plot, it is clear that there were periods after both 8:15 hours and 23:15 hours UTC when the interpolation was much worse than for the rest of the

day. Usually, most discrepancies were less than ± 2.7 cm, and the interpolated ionosphere corrections could be used safely to resolve the ambiguities of the corresponding carrier phase double differences.

Also shown in Fig. 8 is the SRTI index of STEC variability at each station in the network, including the “buoy”, and also at the “rover” STKR. In general, as long as the SRTI < 2 , the residual ddSTEC for STKR is in the “safe” zone of ± 2.7 cm.

Figure 17 shows the SRTI index for STKR, rescaled to correspond to L1, and PKTN for the whole of day 130, comparing it to the often used I95_L index [3]. Notice the elevated ionospheric activity before 8:00 hours, another reason for poor or no corrections available for that earlier period (excluded from this analysis), besides the low precision of the converging Kalman filter. Figures 9 shows the convergence of the navigation filter for the “buoy”, comparing the kinematically determined positions with the precise CORS coordinates for MCON. Likewise, Figures 10 and 11 show the differences in Up, East, and North directions, between the kinematically determined “instantaneous” position of the “rover” (STKR) relative to GALB, and the precise CORS coordinates for STKR.

Ambiguities are solved every time the uncertainty in the “floated” Lc biases exceeds 10 cm. This condition has been forced by re-starting the filter every two hours. One additional re-start, around 8:00 hours, was not planned, but was automatically triggered by too many bad or missing data in STKR during the previous two minutes. Figure 10 also shows the PDOP at each epoch. Figure 11 shows the same discrepancies as in Fig. 10, but to a larger scale, showing more clearly when the successful resolution of three or more ambiguities makes the filter converge abruptly, some 6-12 minutes after each re-start. From Figure 8, it is clear that not many good interpolated ionospheric corrections were available in the period between 8 and 9 hours UTC. Consequently, safety checks in the ambiguity resolution procedure prevented ambiguities from being resolved before 8:45, when the ddSTEC interpolation improved.

Figure 12 shows the effect of TID-induced oscillations on the ddSTEC (PRN 19, with PRN 23 as reference satellite), on day 130, and how they have an adverse effect on the interpolation to PKTN (“truth”, green, interpolated, red).

Figures 13 and 14 show the histograms of the discrepancies between interpolated and “true” ddSTEC for STKR and PKTN, for day 130. For both sites, the rms of the discrepancies for the whole test period was less than 1 cm, and the mean, less than 3 mm. Similar results were obtained for the far more active day 191, with the rms and mean values being about twice as large as those for day 130.

Interpolating the STEC Across Long Data Gaps. Long gaps in reception may require re-starting the navigation filter, followed by a long wait for the filter to converge

once more to the level of precision achieved just before the interruption. As explained in the chapter on Technique, this convergence can be greatly expedited by reconnecting the STEC or ddSTEC. This we have done by fitting a parabola to: (a) the ddSTEC over the 400 seconds previous to a gap, and (b) to its rate of change over a few epochs after the gap. Figure 18 shows the difference between all interpolated and actual ddSTEC for the baseline GALB/MCON, on day 191, a day of high ionospheric activity. Gaps were created artificially every 15 minutes. Plotted in blue and in red, are the results with 2-minute and 5-minute gaps, respectively. Discrepancies of less than 2.7 cm in absolute value should not prevent the correct calculation of changes in the ambiguities of L1 and L2. Clearly, the correct reconnection of phase is more likely after 2 minutes than after five, but still there is a fairly good chance of success with the longer gaps.

Ionospheric Corrections for Use in WAAS/EGNOS-Type Networks.

Here we will discuss briefly the usefulness of having a buoy included in a wide area network supporting a service meant primarily as an aid to civil aviation. The most demanding specifications for such a system concern its use during the final approach and landing of an airplane. Generally speaking, position is expected to be precise at the meter level. The various components of the total error budget (satellite orbit and clock errors, ionosphere and troposphere modeling errors, pseudo-range multipath, etc.) should be small enough that, with reasonable satellite geometry, it should be highly likely that such a precision requirement will be met. One main difference from network-based services for precise (decimeter-level) navigation, such as DGPS or VRS, is that WA services such as WAAS or EGNOS are designed primarily to help users with single-frequency pseudo-range receivers, who need quite precise ionospheric corrections. (In the future, EGNOS might also support very precise positioning with dual-frequency carrier-phase receivers, implementing the WARTK concept [16].) For civil aviation applications such as aircraft approach (Category I), precise approach and landing (Categories II and III), and Local Area Augmentation Systems (LAAS), errors in the ionosphere correction should be less than 40 cm [17].

Using data from the network (sites in black and red) in Figure 1, we have calculated simulated real time corrections for the sites listed in Table 2, below.

TABLE 2

RMS (cm) L1 Correction minus "Truth"		
SITE	Without MCON	With MCON
PKTN	32	16
STKR	34	16
WOOS	38	20
PIT1	55	42

These sites are not part of the wide area network shown in Fig. 1, and lie to the East of the "land" sites, so they can be thought of as "ocean" locations. The Table shows the rms of the differences between the absolute (not differenced) STEC corrections for the L1 frequency, made using the tomographic model, and the STEC calculated off-line with both filter and smoother and the precise site coordinates. Two cases are shown: when the model is created with and without assimilating the "buoy" (MCON) data. The values are for day 130, from 8:30 to 23:30 hours UTC. Figure 19 shows the differences plotted versus time, for all the satellites in view from PKTN (red dots) and STKR (blue dots). Results are very similar for both sites. The addition of the "buoy" clearly improves the quality of the corrections for all the "ocean" sites, and it should improve it also for sites on land located within the perimeter of the extended network

CONCLUSIONS

We have conducted a preliminary feasibility study of the use of buoys with GPS receivers, anchored at some considerable distance from shore, as floating stations of wide area VRS, DGPS, or WA (WAAS, EGNOS) networks, extending them far into the sea. We have concentrated on the ionospheric correction, and in the resolution of carrier phase ambiguities for very precise navigation. But we have also looked into the usefulness of buoys as part of WAAS and EGNOS-type networks for very reliable, meter-level navigation. We have made tests using GPS data from a day when the ionosphere was fairly quiet, and from another day when it was very active. The results are, overall, encouraging. They suggest that buoys with GPS can play an important role as reliable real-time aids to ship and airplane navigation on coastal waters, both at the decimeter and at the meter-level of precision.

ACKNOWLEDGEMENTS

The authors are grateful to the International GPS Service and cooperating organizations, such as CORS, for making publicly available its data sets and products. This work has been partially supported by the Spanish project ESP-2004-05682-C02-01 and the GJU project WARTK-EGAL.

REFERENCES

- [1] Chen, X., H. Landau, U. Vollath: "New Tools for Network RTK Integrity Monitoring." Proceedings of the ION GPS/GNSS 2003, pp. 1355-1360, Portland, Oregon, 2003.
- [2] Rizos, C., S. Han: "Reference Station Network Based RTK Systems – Concepts and Progress." 4th International GPS/GNSS Symposium Wuhan, P.R. China, CD-ROM Proceedings, 2002.

- [3] Wanninger, L.: "The Performance of Virtual Reference Stations in Active Geodetic GPS-Networks under Solar Maximum Conditions." Proceedings of ION GPS 99, Nashville, TN, 1419-1427, 1999.
- [4] C. Kee, "Wide Area Differential GPS," in B. Parkinson and J. Spilker, Eds., *Global Positioning System: Theory and Applications*. AIAA, Progress in Astronautics and Aeronautics series, Volume II, Chapter 3, pp. 81-114, 1996.
- [5] Enge, P., et.al.: "Wide Area Augmentation of the Global Positioning System," *Proceedings of the IEEE*. Vol. 84, No. 8, pp. 1063-1089, August 1996.
- [6] Kato, T.: "A New Tsunami Monitoring System Using RTK-GPS", in Proceedings of the International Tsunami Symposium 2001, Session 5, Number 5-12, 645-651, 2001.
- [7] Kato, T., Y. Terada, K. Ito, R. Hattori, T. Abe, T. Miyake, S. Koshimura, T. Nagai: "Tsunami due to the 2004 September 5th Off Kii Peninsula Earthquake, Japan, Recorded by a New GPS Buoy", in *Earth, Planets and Space*, (in printing), 2005
- [8] White, N.J., R. Coleman, J.A. Church, P.J. Morgan and S.J. Walker: "A Southern Hemisphere Verification for the Topex/Poseidon Satellite Altimeter Mission." *J. Geophys. Res.*99, 24505-24516, 1994.
- [9] White, N.J., R. Coleman, J.A. Church, C. Watson, G. Musiela, and R. Govind: "Jason-1 Verification in Bass Strait and at Other Sites in the Australian Region", JASON-1 Cal-Val Plan, CNES Report TP2-J0-PL-974-CN, Toulouse, 2001.
- [10] Colombo, O.L., M. Hernandez-Pajares, J.M. Juan, J. Sanz, and J. Talaya: "Resolving Carrier-phase Ambiguities On-The-Fly, at More than 100 km from Nearest Site, with the Help of Ionospheric Tomography", Proceedings ION GPS'99, Nashville, Tennessee, USA, September 1999.
- [11] Hernandez-Pajares M., J. M. Juan and J. Sanz: "Improving the Real-Time Ionospheric Determination from GPS Sites at Very Long Distances Over the Equator", *Journal of Geophysical Research*, Vol. 107, No. A10, 1296, doi:10.1029/2001JA009293, 2002.
- [12] Colombo, O.L., M. Hernandez-Pajares, J.M. Juan, J. Sanz: "Wide-Area, Carrier-Phase Ambiguity Resolution Using a Tomographic Model of the Ionosphere", *Navigation, J. ION.*, Vol.49, No.1, Spring 2002.
- [13] Colombo, O.L., A.G. Evans, M. Ando, K. Tadokoro, K. Sato, T. Yamada: "Speeding Up The Estimation Of Floated Ambiguities For Sub-Decimeter Kinematic Positioning At Sea", Proceedings ION GPS-2001, Salt Lake City, September 2001.
- [14] Hernandez-Pajares, M. Juan, J.M. Sanz, J. Colombo, O.L.: "Impact of Real-Time Ionospheric Determination on Improving Precise Navigation with GALILEO and Next-Generation GPS", *Navigation, J. Inst. Navig.*, Alexandria, Vol. 50, No. 3, Fall Issue, 2003.
- [15] Colombo, O.L., A. Sutter, A.G. Evans: "Evaluation of Real-Time, Long-Range, Precise, Differential, Kinematic GPS Using Broadcast Orbits", Proceedings ION GNSS-2003, Portland, Oregon, September 2003.
- [16] Hernandez-Pajares, M. Juan, J.M. Sanz, J. Orús, R., Garcia, A., O.L. Colombo: "Wide Area Real Time Kinematics with Galileo and GPS Signals", Proceedings ION GNSS-2004, pp. 205-218, Long Beach, California, 2004.
- [17] Walter, T., S. Datta-Barua, J. Blanch, and P. Enge: "The Effects of Large Ionospheric Gradients on Single Frequency Airborne Smoothing Filters for WAAS and LAAS", Proceedings ION NTM 2004.
- [18] Muellerschoen, R.J., W.I. Bertiger, M.F. Lough: "Results of an Internet-Based Dual-Frequency Global Differential GPS System", Proceedings ION 2000 Annual Technical Meeting, 2000.
- [19] Muellerschoen, R.J., A. Reichert, D. Kuang, M. Heflin, W.I. Bertiger, Y. Bar-Server: "Orbit Determination with NASA's High Accuracy Real-Time Global Differential GPS System", Proceedings ION GPS 2001.
- [20] Hatch, R., T. Sharpe, P. Galyean: "StarFire: A Global High Accuracy Differential GPS System", Proceedings of GPS Symposium 2002, Japan Institute of Navigation, 2002.